High-resolution rotational analysis of HDS: $2v_3$, $v_2 + 2v_3$, $3v_3$, and $v_2 + 3v_3$ bands

A.-W. Liu [a], B. Gao [a], G.-S. Cheng [a], F. Qi [b], S.-M. Hu [a,*]

[a] *Hefei National Laboratory for Physical Sciences at Microscale, Department of Chemical Physics,
University of Science and Technology of China, Hefei 230026, China*
[b] *National Synchrotron Radiation Laboratory, University of Science and Technology of China, Hefei 230027, China*

Abstract

High-resolution Fourier transform spectrum of the $HD^{32}S$ molecule was studied in the region of 5000–9000 cm^{-1}. More than 1600 observed transitions yielded 239, 264, 131, and 116 upper state ro-vibrational energies of the states (002), (012), (003), and (013), respectively. With a Watson-type effective Hamiltonian model, the ro-vibrational parameters of these four upper states were determined by a least-square fitting which can reproduce the ro-vibrational energies close to the experimental accuracy. The relative linestrengths are also discussed.
© 2005 Elsevier Inc All rights reserved.

1. Introduction

Besides the fundamental interest of the hydrogen sulfide molecule, the knowledge of hydrogen sulfide absorption spectra is also important for the study on the atmosphere of planets (like Venus) and interstellar medium [1], and for terrestrial remote sensing applications. In the last few decades, the absorption spectra of H_2S have been studied extensively, with microwave [2–6], Fourier-transform infra-red [7–13], and intra-cavity laser absorption spectroscopy at near-IR and visible region [14–21]. But for the deuterated sample, there are just a few bands were studied with high-resolution. The fundamental and $v_1 + v_2/v_2 + v_3$ bands of doubly deuterated hydrogen sulfide studied by Camy-Peyret et al. [22] and Ulenikov et al. [23], respectively. The mono-deuterated hydrogen sulfide has been inves-

tigated up to 4000 cm^{-1}. Ulenikov et al. studied the bands $v_1 + v_2/v_3$ [23], $nv_2(n = 1, 2, 3)$ [24–26], and v_1 and $2v_1/v_2 + v_3$ [27]. Several empirical determinations of the potential energy surface (PES) of hydrogen sulfide have been performed [28–31], and a deviation of 0.03 cm^{-1} of numerical energy calculations including variant isotopes was achieved by Tyuterev et al. [32]. High-level ab initio calculations on PES and dipole moment surfaces (DMS) with large basis sets have also been reported [33–35]. The intensity anomalies in the ro-vibrational spectra also attracted great interest, see [32] for example.

The present work is devoted to the high-resolution Fourier-transform spectroscopy study of HDS in the infrared region, continuing our previous studies [9,10] on the high-resolution ro-vibrational spectroscopy of the hydrogen sulfide molecule ($H_2S/HDS/D_2S$). The experimental details are presented in Section 2. The analysis of the $2v_3$, $v_2 + 2v_3$, $3v_3$, and $v_2 + 3v_3$ bands are given in Section 3.

2. Experimental details

Deuterated hydrogen sulfide sample was synthesized with diluted phosphoric acid and sodium sulfide. The phosphoric acid-d3 (85% solution in D_2O, >99% D atom, from Fluka Chemical) was further diluted with deuterated water (99.8%, from PeKing Chemical Industry). Anhydrous sodium sulfide (99.9%) was purchased from Acrōs Organics. The synthesized gas was collected and purified with low temperature distillations. The spectra were recorded at room temperature with a Bruker IFS 120HR Fourier transform spectrometer equipped with a path length adjustable multi-pass gas cell. A tungsten source and a CaF_2 beam-splitter were used. Because of the wide spectral range and the large variation of the absorption line intensities, different experimental conditions were used in the measurements as listed in Table 1. For two measurements with the conditions given in the last two lines of that table, the isotope abundance in the synthesized sample was also measured by a photoionization mass spectrum (PIMS) experiment. PIMS was measured at the photon energy of 11 eV with a re-electron time-of-flight mass spectrometer in the photochemistry endstation of National Synchrotron Radiation Laboratory, Hefei. It gave the following abundance in the sample: $H_2^{32}S$ 3.0%, $HD^{32}S$ 23.5%, $D_2^{32}S$ 68.7%, $D_2^{33}S$ 0.5%, $HD^{34}S$ 1.0%, and $D_2^{34}S$ 3.0%. And no optical filter was used to avoid fringes in the baseline, which helps to obtain the linestrengths values. In other measurements which are mainly toward the accurate determination of the line positions, optical filters were applied to increase both the signal-noise-ratio and the resolution. An overview of the spectrum is given in Fig. 1 and parts of spectra are also presented in Figs. 2 and 3. The line positions were calibrated using H_2O and CO_2 lines listed in

Table 1
Experimental conditions used to record the Fourier-transform absorption spectra of the synthesized sample

Region (cm^{-1})	Gas pressure (Pa)	Detector	Path length (m)	Number of scans	Resolution (cm^{-1})
3400–4200	4445	InSb	87	2768	0.010
4000–5200	8043	InSb	87	1343	0.008
4000–5200	2997	InSb	51	1507	0.008
4900–6400	4445	Ge	105	2055	0.008
2000–9000[a]	1883	InSb	69	2532	0.016
5000–9000[a]	8043	Ge	105	2954	0.016

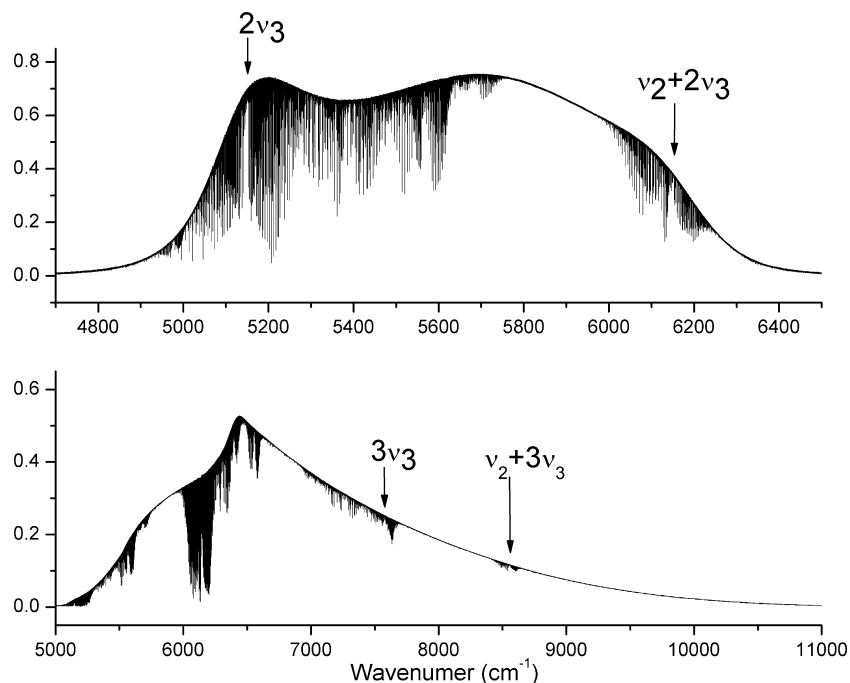[a] The abundance of this sample was given by the mass spectroscopy.

Fig. 1. Overview spectrum of the synthesized HDS/D_2S/H_2S sample in the region 4700–9000 cm^{-1}. Experimental conditions: (upper panel) absorption path length 105 m, sample pressure 4445 Pa, unapodized resolution 0.008 cm^{-1}; (lower panel) absorption path length 105 m, sample pressure 8033 Pa, unapodized resolution 0.016 cm^{-1}.
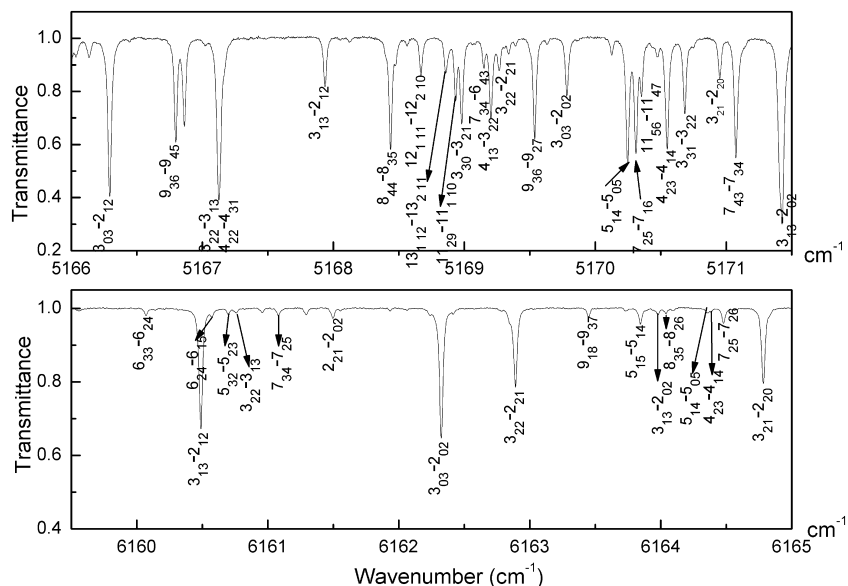
Fig. 2. A small part of the HDS spectrum. (Upper panel) 5166–5171.5 cm^{-1} region of the $2\nu_3$ band. (Lower panel) 6159.5–6165 cm^{-1} of the $\nu_2 + 2\nu_3$ band. Experimental conditions: absorption path length 69 m, sample pressure 1883 Pa, unapodized resolution 0.016 cm^{-1}, isotope abundance of HD^{32}S, 23.5%, room temperature.
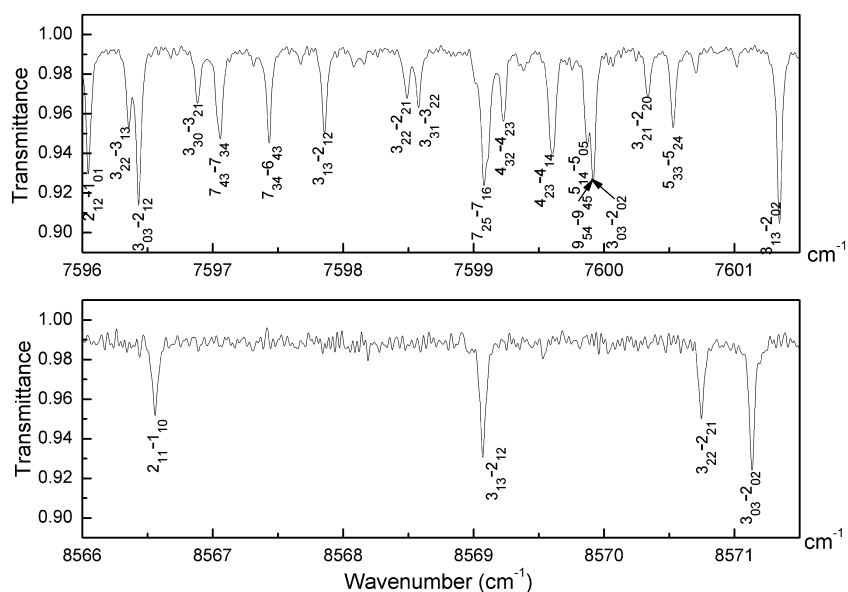
Fig. 3. A small part of the HDS spectrum. (Upper panel) 7596–7601.5 cm^{-1} region of the $3\nu_3$ band. (Lower panel) 8566–8571.5 cm^{-1} region of the $\nu_2 + 3\nu_3$ band. Experimental conditions: absorption path length 105 m, sample pressure 8033 Pa, unapodized resolution 0.016 cm^{-1}, isotope abundance of HD^{32}S, 23.5%, room temperature.

Table 2
General information on studied vibrational states of HD^{32}S

$v_1 v_2 v_3$	Band center (cm^{-1})		J^{max}	K_a^{max}	Number of transitions	Number of energy levels
	Calc., Ref. [29]	This work				
(0 0 2)	5147.97	5147.36	23	11	885	239
(0 1 2)	6141.30	6139.73	20	11	664	264
(0 0 3)	7578.22	7577.84	20	7	516	131
(0 1 3)	8550.18	8548.89	17	6	208	116

Table 3
Experimental ro-vibrational energy levels of the (002), (012), (003), and (013) vibrational states of HDS (in cm^{-1})[a]

J	K_a	K_c	(002) E	Δ	δ	(012) E	Δ	δ	(003) E	Δ	δ	(013) E	Δ	δ
	1		2	3	4	5	6	7	8	9	10	11	12	13
0	0	0	5147.3553	2	1	6139.7315	0	1	7577.8430	0	−23	8548.8927	0	−13
1	0	1	5155.4545	7	−1	6147.8925	1	2	7585.9094	5	3	8557.0222	48	21
1	1	1	5159.6988	3	5	6152.2922	2	5	7589.8673	10	6	8561.1205	20	34
1	1	0	5161.4626	7	2	6154.1867	1	0	7591.6624	12	3	8563.0523	26	−6
2	0	2	5171.2058	4	4	6163.7221	0	0	7601.5596	11	5	8572.7523	8	6
2	1	2	5174.1294	13	−8	6166.7149	0	2	7604.2048	27	4	8575.4557	5	5
2	1	1	5179.4177	8	−1	6172.3955	2	−2	7609.5897	28	−18	8581.2377	6	0
2	2	1	5192.1473	15	−8	6185.5875	1	2	7621.4582	7	2	8593.5285	21	6
2	2	0	5192.5904	5	1	6186.0778	1	1	7621.9415	12	8	8594.0638	4	−2
3	0	3	5193.8771	3	2	6186.4185	1	1	7624.0136	19	18	8595.2335	51	−52
3	1	3	5195.5210	9	4	6188.0723	2	3	7625.4380	18	9	8596.6559	28	−5
3	1	2	5206.0230	6	0	6199.3459	1	−2	7636.1155	12	−1	8608.1164	7	5
3	2	2	5216.4119	4	4	6210.0362	2	3	7645.6337	10	−8	8617.8945	31	−11
3	2	1	5218.4730	9	7	6212.3040	1	−3	7647.8577	7	11	8620.3408	7	4
3	3	1	5242.2699	8	−3	6237.0120	0	1	7670.1607	14	−11	8643.4748	14	−5
3	3	0	5242.3413	5	5	6237.0943	2	−1	7670.2445	3	−1	8643.5721	27	−13
4	0	4	5222.8821	2	2	6215.3622	1	1	7652.7000	12	10	8623.8458	7	1
4	1	4	5223.6630	9	−1	6216.1315	4	−1	7653.3422	12	11	8624.4753	15	5
4	1	3	5240.7900	5	−4	6234.4937	0	−4	7670.7006	23	4	8643.0823	10	4
4	2	3	5248.4143	5	1	6242.2467	2	−2	7677.4812	35	3	8649.9564	8	−14
4	2	2	5253.8361	11	−2	6248.1790	1	−3	7683.2617	6	4	8656.2794	12	−15
4	3	2	5275.2827	16	0	6270.3322	0	−1	7703.1043	7	−5	8676.7394	10	3
4	3	1	5275.7697	9	0	6270.8838	4	4	7703.6718	15	1	8677.3837	10	6
4	4	1	5310.5056	5	1	6307.0188		3	7736.3984	22	−28	8711.4011[b]		−97
4	4	0	5310.5167	12	−14	6307.0310		−8	7736.4073	7	5	8711.4065[b]		−93
5	0	5	5258.0412	3	3	6250.3797	8	−8	7687.4752	29	11	8658.4781	33	−47
5	1	5	5258.3711	6	−1	6250.6966	3	1	7687.7335	20	1	8658.7201	0	0
5	1	4	5282.9746	2	−1	6277.0169	1	−5	7712.5323	15	−6	8685.2373	13	6
5	2	4	5287.8696	6	3	6281.9075	1	0	7716.6976	13	2	8689.3785	7	3
5	2	3	5298.5101	7	−4	6293.4927	0	−6	7727.9091	16	1	8701.5767	12	24
5	3	3	5316.5823	7	−2	6312.0113	1	0	7744.2990	4	1	8718.3288	15	5
5	3	2	5318.3806	7	0	6314.0398	0	−1	7746.3706	9	0	8720.6644	30	8
5	4	2	5351.7684	7	2	6348.6682	1	2	7777.5926	18	−3	8753.0011	19	−1
5	4	1	5351.8529	9	5	6348.7664	3	7	7777.6996	5	−6	8753.1270	30	−14
5	5	1	5396.9208	4	−12	6395.6694	16	11	7820.2357	24	9	8797.3673	46	0
5	5	0	5396.9214	8	−6	6395.6726	22	−7	7820.2358	22	25	8797.3705	8	−13
6	0	6	5299.3926	7	2	6291.5170	4	−3	7728.3958	25	−14	8699.1736	3	0
6	1	6	5299.5213	5	1	6291.6374	4	7	7728.4900	8	−2	8699.2618	2	12
6	1	5	5331.7532	4	1	6326.0285	0	−3	7760.7661	4	4	8733.6857	22	−13
6	2	5	5334.4699	5	2	6328.6833	3	2	7762.9568	25	−4	8735.8092	17	5
6	2	4	5351.9569	9	2	6347.6386	0	−6	7781.1852	5	−1	8755.5533	11	12
6	3	4	5366.0024	9	−1	6361.8616	1	0	7793.5502	22	2	8768.0224	19	−4
6	3	3	5370.6932	6	0	6367.1106	1	−4	7798.8480	14	−13	8773.9405	25	10
6	4	3	5401.5154	16	13	6398.9014	8	−4	7827.2720	28	−10	8803.1904	39	−15
6	4	2	5401.9223	4	5	6399.3733	1	0	7827.7792	19	−4	8803.7812	48	−11
6	5	2	5446.2533	25	−10	6445.4515	11	−46	7869.4961	45	−57			
6	5	1	5446.2649	3	−3	6445.4547[b]		70	7869.5011[b]	31	66	8847.1051	46	53
6	6	1	5501.4592	1	−8	6502.8989	2	5	7921.6311	11	22	8901.3304	9	0
6	6	0	5501.4589	3	−4	6502.8992	3	3		21	9	8901.3308	13	−1
7	0	7	5346.9961	14	−13	6338.8401	22	−20	7775.5137	19	−16	8746.0054	23	9
7	1	7	5347.0418	7	6	6338.8791	26	29	7775.5446	11	10	8746.0369	5	0
7	1	6	5386.5997	9	−3	6380.9976	0	−3	7814.9496	11	10	8787.9752	19	−8
7	2	6	5387.9243	11	−3	6382.2613	11	5	7815.9598	17	−9	8788.9281	12	7
7	2	5	5413.4068	5	−5	6409.7587	0	−5	7842.2321	19	−1	8817.2521	11	−11
7	3	5	5423.2751	7	2	6419.5848	4	−3	7850.5568	23	−9	8825.4790	36	30
7	3	4	5432.8474	6	−4	6430.1978	3	−1	7861.1272	17	−9	8837.1831	4	16
7	4	4	5459.7574	4	5	6457.7186	1	3	7885.4186	16	21	8861.9385	21	17
7	4	3	5461.1394	6	4	6459.3175	1	1	7887.1243	8	6	8863.9099	32	17
7	5	3	5504.0755	11	−2	6503.8164	3	4	7927.2446	13	11	8905.4279	29	−40

Table 3 (continued)

J	K_a	K_c	(002)			(012)			(003)			(013)		
			E	Δ	δ	E	Δ	δ	E	Δ	δ	E	Δ	δ
	1		2	3	4	5	6	7	8	9	10	11	12	13
7	5	2	5504.1475	7	5	6503.9033	3	4	7927.3421	18	19	8905.5325[b]		−94
7	6	2	5558.7637	13	−15	6560.6906	13	9	7978.8395	14	−4	8959.0538	4	−7
7	6	1	5558.7630	18	9	6560.6922	15	13	7978.8406	43	9	8959.0554	31	6
7	7	1	5624.0369	7	−5	6628.6010	1	2	8040.4997	2	−14			
7	7	0	5624.0371	5	−7	6628.6011	0	2	8040.4997	3	−14			
8	0	8	5400.8811	10	−18	6392.3760	5	−2	7828.8587	12	−17	8798.9976	10	18
8	1	8	5400.8945	22	17	6392.3900	6	9	7828.8684	20	−2	8799.0104	8	−9
8	1	7	5447.4118	4	−3	6441.8502	5	−5	7875.0562	20	−13	8848.1035	24	36
8	2	7	5447.9970	7	0	6442.3954	2	1	7875.4757	22	2	8848.4962	30	−3
8	2	6	5481.9218	6	−2	6478.8290	4	2	7910.0540	19	−16	8885.5870	7	−13
8	3	6	5488.0667	14	−2	6484.8120	1	0	7914.9523	19	0	8890.3093	13	17
8	3	5	5504.4409	10	5	6502.8150	21	17	7932.6728	22	2	8909.7640	4	−11
8	4	5	5526.3947	13	1	6525.0049	3	2	7951.9097	15	−10	8929.1004	8	−26
8	4	4	5530.0541	10	5	6529.2016	1	2	7956.3202	14	2	8934.1535	45	−49
8	5	4	5570.4785	10	0	6570.8763	1	6	7993.5915	21	4	8972.4651	21	−19
8	5	3	5570.7802	5	3	6571.2361	3	8	7993.9986	16	−15	8972.9544[b]		73
8	6	3	5624.5103	26	−28	6627.0298		−49	8044.5001	54	4			
8	6	2	5624.5168	25	47	6627.0305[b]		82	8044.5133	47	35			
8	7	2	5689.2167	14	−2	6694.3020	2	7						
8	7	1	5689.2164	8	1	6694.3022	1	8						
8	8	1	5764.5520	9	4	6772.6532	5	4						
8	8	0	5764.5520	8	4	6772.6532	4	4						
9	0	9	5461.0598	19	−24	6452.1399	6	8	7888.4363	2	6	8858.1605		4
9	1	9	5461.0599	23	32	6452.1459	7	−2	7888.4375	20	31	8858.1605		36
9	1	8	5514.2862	8	−1	6584.1006	0	1	8012.6016	5	15			
9	2	8	5514.5267	3	2	6508.9199	28	−21	7941.3577	7	2	8914.3576	19	9
9	2	7	5556.6520	4	0	6553.9634	0	−1	7983.8483	16	−8	8959.7462	4	−14
9	3	7	5560.0233	8	−2	6557.1622	2	2	7986.3716	17	−9			
9	3	6	5584.7078	4	−3	6508.6959	6	26	7941.1926	11	15	8914.2099		12
9	4	6	5601.2111	5	0	6600.5118	4	2	8026.4739	6	2	9004.3632	17	14
9	4	5	5609.0871	21	−6	6609.4375	2	1	8035.6900	29	15	9014.7859	20	−39
9	5	5	5645.5071	12	13	6646.6712	1	3	8068.5591	23	5	9048.2296	10	36
9	5	4	5646.4965	19	−3	6647.8430	2	1	8069.8677	36	−7	9049.7852	7	−11
9	6	4	5698.7930	6	1	6702.0081	9	10	8118.7252	27	−6			
9	6	3	5698.8472	7	7	6702.0759	8	2						
9	7	3	5762.7831	10	−22	6768.4827	11	6						
9	7	2	5762.7817	18	7	6768.4837	8	15						
9	8	2	5837.5004	11	18	6846.1456	11	3						
9	8	1	5837.5005	9	16	6846.1456	11	3						
9	9	1	5922.8899	14	15	6934.9210	6	−15						
9	9	0	5922.8899	14	15	6934.9207	3	−12						
10	0	10	5527.5314	0	−20	6518.1300	30	33	7954.2518	46	−10	8923.4906		−8
10	1	10	5527.5298	15	15	6518.1373	26	−24	7954.2550	26	−31	8923.4906		1
10	1	9	5672.6604	5	18	6672.9604	2	8	8099.8334	6	−1	9078.7655		−49
10	2	9	5587.4168	4	−5	6581.7317	1	1	8013.5188	17	13	8986.4342	3	−11
10	2	8	5637.1676	9	2	6634.7670	19	−32	8063.3258	17	19	9039.4811	8	43
10	3	8	5638.8227	7	−1	6636.2936		1	8064.4869	26	31	9040.5461	43	−4
10	3	7	5587.3239	22	−14	6581.6483		1	8013.4595	0	3	8986.3793	48	9
10	4	7	5683.8887	12	13	6683.8848	1	3	8108.7603	43	−38	9087.3416	26	−14
10	4	6	5698.1530	11	−1	6699.8522	1	3	8124.9514	8	13	9105.4092	49	48
10	5	6	5729.1266	9	15	6731.1476	7	9	8152.0779	42	−18	9132.6393		5
10	5	5	5731.7905	6	3	6734.2798	4	2	8155.5235	4	−18	9136.6828		14
10	6	5	5781.7155	11	1	6785.7482	4	8						
10	6	4	5781.9254	3	9	6786.0054	4	8						
10	7	4	5844.8201	22	−35	6851.2450	1	−48						
10	7	3	5844.8227	10	27	6851.2455[b]		56						
10	8	3	5918.7784	6	−11	6928.0544	7	8						
10	8	2	5918.7795	12	2	6928.0545	5	9						
10	9	2	6003.4910		14	7016.0715	1	−3						
10	9	1	6003.4910		14	7016.0715	1	−3						

Table 3 (*continued*)

J	K_a	K_c	(002) E	Δ	δ	(012) E	Δ	δ	(003) E	Δ	δ	(013) E	Δ	δ
	1		2	3	4	5	6	7	8	9	10	11	12	13
10	10	1	6098.9284		−42	7115.2496		0						
10	10	0	6098.9284		−42	7115.2496		0						
11	0	11	5600.2923	9	−15	6590.3482	12	12	8026.2940	17	−5	8994.9817	18	−6
11	1	11	5600.2900	12	13	6590.3508	9	−10	8026.2937	17	1	8994.9817	18	−3
11	1	10	5767.2481		−4	6768.2626	6	10	8193.2936	11	−2	9172.8620		18
11	2	10	5666.6122	9	−1	6660.7864	8	−6	8091.9161	7	20			
11	2	9	5796.6152		0	6799.6854	0	18						
11	3	8	5666.5785	15	−14	6660.7549	6	7				9064.6587	17	9
11	3	9	5724.2108	8	−2	6721.9427	7	−6	8149.0701	19	12			
11	4	8	5774.0553	18	1	6774.7133	13	−10	8198.3560	45	4			
11	4	7	5723.4655	14	3	6721.2731	23	−20	8148.5788	18	6			
11	5	7	5821.1855	8	9	6824.1263	1	7	8243.9338	23	32			
11	5	6	5827.2196	6	8	6831.1347	4	1	8251.4954	30	−13			
11	6	6	5873.3455	15	13	6878.3180	1	−1						
11	6	5	5874.0214	5	−5	6879.1374	9	−2						
11	7	5	5935.4193	3	3	6942.6808	9	−6						
11	7	4	5935.4602	22	−21	6942.7283	10	0						
11	8	4	6008.4580	12	1	7018.4639	15	5						
11	8	3	6008.4575	16	18	7018.4648	1	12						
11	9	3	6092.3659	33	−18	7105.5767	7	8						
11	9	2	6092.3662	30	−20	7105.5767	6	8						
11	10	2	6187.0477	17	−3	7203.9174	1	−4						
11	10	1	6187.0477	17	−3	7203.9174	1	−4						
11	11	1	6292.5044		19									
11	11	0	6292.5044		19									
12	0	12	5679.3340	8	4	6668.7816	5	4	8104.5574	8	3	9072.6277	14	2
12	1	12	5679.3340	8	6	6668.7826	3	−4	8104.5574	8	4	9072.6277	14	3
12	1	11	5933.0573		3	6938.6160		13						
12	2	11	5752.0827	16	26	6746.0542	6	−8				9149.0717		−14
12	3	10	5816.0128	17	−9	6813.9319	1	1	8239.9627	11	−19	9216.4240		47
12	3	9	5752.0753		−25	6746.0430	7	−2	8176.5237	41	−19	9149.0685	10	−33
12	4	9	5871.3232	22	17	6872.5838	6	−3				9274.6805		−53
12	4	8	5815.6988	0	−6	6813.6557		9	8239.7655	45	4			
12	5	8	5921.4114	12	8	6925.2966	13	−7						
12	5	7	5867.6477	14	2	6869.2050		−57						
12	6	7	5973.6978	10	−7	6979.7164	2	3						
12	6	6	5975.5438	7	−2	6981.9418	11	9						
12	7	6	6034.6877	4	8	7042.9104	14	14						
12	7	5	6034.8299		−4	7043.0876	8	3						
12	8	5	6106.6233	6	−21	7117.4722	2	−51						
12	8	4	6106.6310		−35	7117.4725	22	26						
12	9	4	6189.5674	26	27	7203.5108		−4						
12	9	3	6189.5683	13	19	7203.5107		−1						
12	10	3	6283.3831		8	7300.8754	13	9						
12	10	2	6283.3831		8	7300.8754	13	9						
12	11	2				7409.5119		7						
12	11	1				7409.5119		7						
13	0	13	5764.6525	4	−3	6753.4236	3	−3	8189.0356	9	−5	9156.4237	27	−15
13	1	13	5764.6525	4	−2	6753.4236	3	−2	8189.0362	15	−11	9156.4237	27	−15
13	1	12				7056.2532	0	11						
13	2	12	5843.8186	19	8	6837.5189	9	1						
13	2	11				7023.0338	4	12				9426.4791		2
13	3	11	5914.1218	10	−17	6912.1606	0	−3	8337.0727	0	−13			
13	3	10	5843.8149	27	1	6837.5163	24	−9				9239.5981	9	8
13	4	10	5975.3610	16	−7	6977.1489	9	−42						
13	4	9	5913.9960	9	−10	6912.0522	8	10	8336.9999	0	−17			
13	5	9	6029.4388	8	16	7034.2471	2	3						
13	5	8	5973.5639	5	−13	6975.5350	0	15						
13	6	8	6082.6823		−14	7089.8310	14	16						
13	6	7				7095.0432	14	−14						

Table 3 (continued)

J	K_a	K_c	(002) E	Δ	δ	(012) E	Δ	δ	(003) E	Δ	δ	(013) E	Δ	δ
	1		2	3	4	5	6	7	8	9	10	11	12	13
13	7	7	6142.7114		−18	7152.0278	19	−18						
13	7	6	6143.1570	4	−13	7152.5821	26	−15						
13	8	6	6213.3620		−9	7225.1662	24	6						
13	8	5	6213.3919		−51	7225.2000	8	−2						
13	9	5	6295.1812		−2	7309.9531	4	−25						
13	9	4	6295.1789	0	30	7309.9535	11	−16						
13	10	4	6387.9885		6	7406.1906		4						
13	10	3	6387.9884		7	7406.1906		4						
13	11	3	6491.6777		−12	7513.7710		−10						
13	11	2	6491.6777		−12	7513.7710		−10						
14	0	14	5856.2347	2	−2	6844.2648	1	−4	8279.7151	9	12	9246.3565	4	−15
14	1	14	5856.2347	2	−1	6844.2648	1	−4	8279.7162	24	1	9246.3565	4	−15
14	1	13	6174.0813		0	7183.0189	8	−15						
14	2	13	5941.7998	6	18	6935.1747	23	−30						
14	2	12	6209.0685	13	−31	7218.9370		7						
14	3	12	6018.4781	12	−15	7016.5710		11						
14	3	11	5941.7994	8	8	6935.1675	32	31						
14	4	11	6085.9023	13	−18	7088.1313	6	−3						
14	4	10	6018.4318	14	−29	7016.5283		4						
14	5	10	6144.8573	8	−8	7150.5332		−10						
14	5	9	6085.0888	19	−8	7087.4224	7	17						
14	6	9				7208.4162		4						
14	6	8	6137.8881	14	−9	7144.1191		−7						
14	7	8				7270.0650	6	−12						
14	7	7	6260.7665	28	15									
14	8	7	6328.7716	24	39	7341.6699	16	20						
14	8	6				7341.7892	5	−2						
14	9	6				7424.9896	2	−13						
14	9	5	6409.2821	13	−11	7424.9890	6	47						
14	12	3				7744.0705	18	0						
14	12	2				7744.0705	18	0						
15	0	15	5954.0716	3	−2	6941.2962	1	−8	8376.5909	14	3	9342.4164	4	2
15	1	15	5954.0716	3	−2	6941.2962	1	−8	8376.5909	14	3	9342.4164	4	2
15	1	14				7317.5863		2						
15	2	14	6046.0191	15	22	7039.0022	14	−7				9439.0321		−18
15	2	13	6341.6461		12	7353.5694		−4						
15	3	13				7127.1381		6						
15	3	12	6046.0222	5	−14	7039.0002	8	10				9439.0274		28
15	4	12				7205.3693	1	0						
15	4	11	6129.0314	9	3	7127.1202	25	43						
15	5	11	6267.2582		39	7273.7235	6	−9						
15	5	10	6202.4249	11	−11	7205.0749		24						
15	6	10				7335.0932		4						
15	6	9				7270.4337		−33						
15	7	9				7396.9736		5						
15	8	7				7467.4521		−20						
16	0	16	6058.1513	9	6	7044.5055	9	4	8479.6490	0	−1	9444.5915		50
16	1	16	6058.1513	9	6	7044.5055	9	4	8479.6490	0	−1	9444.5915		50
16	2	15	6156.4664	8	5	7148.9993	2	−10						
16	3	14				7243.8447	9	−14						
16	3	13	6156.4668	1	−1	7148.9984	9	−1						
16	4	13				7328.7588		13						
16	4	12	6245.8113	37	13	7243.8377	3	8						
16	5	12	6396.3072		−2	7403.4639		−8						
16	5	11	6325.7206		−7	7328.6430		23						
16	6	11				7469.4028		27						
16	6	10				7401.9183		0						
17	0	17	6168.4656		−13	7153.8847	7	0	8588.8768	0	10	9552.8865		−28
17	1	17	6168.4656		−13	7153.8847	7	0	8588.8768	0	10	9552.8865		−28
17	2	16	6273.1242	14	28	7265.1496	12	19						

Table 3 (*continued*)

J	K_a	K_c	(002)			(012)			(003)			(013)		
			E	Δ	δ	E	Δ	δ	E	Δ	δ	E	Δ	δ
	1		2	3	4	5	6	7	8	9	10	11	12	13
17	2	15				7651.3727		0						
17	3	15	6368.7680	10	33	7366.6769	8	−30						
17	3	14	6273.1243	16	26	7265.1497	10	17						
17	4	14	6455.1085	12	38	7458.2501		−5						
17	4	13	6368.7692	18	0	7366.6715	15	8						
17	5	13				7539.5002		−32						
17	6	11				7538.8194		26						
18	0	18	6284.9971	13	−9	7269.4194	15	8	8704.2640	0	14			
18	1	18	6284.9971	13	−9	7269.4194	15	8	8704.2640	0	14			
18	2	17	6395.9893	17	−3	7387.4504		−11						
18	3	15	6395.9893	17	−3	7387.4502		−9						
18	4	15				7593.8127		−17						
18	4	14	6497.8971	12	−36	7495.6213		−24						
18	5	14				7681.6607		10						
18	5	13				7593.7952		4						
18	6	12				7681.3821		14						
19	0	19	6407.7329	18	18	7391.1003	1	−7	8825.8025	0	−35			
19	1	19	6407.7329	18	18	7391.1003	1	−7	8825.8025	0	−35			
19	2	18				7515.8799		−2						
19	3	17				7630.6678		3						
19	3	16				7515.8798		−1						
19	4	15				7630.6647		32						
19	5	14				7735.4262		−41						
20	0	20	6536.6650		9	7518.9096		4	8953.4629	0	14			
20	1	20	6536.6650		9	7518.9096		4	8953.4629	0	14			
20	2	19				7650.4308		−10						
20	3	17				7650.4308		−10						
20	4	16				7771.8051		25						
21	0	21	6671.7776		−22									
21	1	21	6671.7776		−22									
22	0	22	6813.0483		−5									
22	1	22	6813.0483		−5									
23	0	23	6960.4667		9									
23	1	23	6960.4667		9									

[a] Δ is the experimental uncertainty of the energy value, equal to one standard deviation, in units of 10^{-4} cm^{-1}, Δ is not quoted when the energy value was obtained from only one transition. $\delta = E^{\mathrm{exp}} - E^{\mathrm{calc}}$, also in units of 10^{-4} cm^{-1}.

[b] The energy levels are not included in the parameters fitting.

HITRAN database [36]. The accuracy of line positions of unblended and not-very-weak lines was estimated to be better than 0.002 cm^{-1}.

3. Spectral analysis and results

Because the HDS molecule is an asymmetric top with C_s symmetry, any of its vibrational–rotational bands include both 'A' and 'B' type transitions ('A' and 'B' bands). As a consequence, the selection rules are

$$\Delta J = 0, \pm 1; \quad \Delta K_a = 0, \pm 2, \pm 4 \ldots;$$
$$\Delta K_c = \pm 1, \pm 3 \ldots, \tag{1}$$

for 'A' type transitions, and

$$\Delta J = 0, \pm 1; \quad \Delta K_a = \pm 1, \pm 3 \ldots;$$
$$\Delta K_c = \pm 1, \pm 3 \ldots, \tag{2}$$

for 'B' type transitions. These selection rules were used in spectral assignments based on the ground state combination differences (GSCD). The ground state rotational energies were calculated with the parameters from [2]. The statistical results of the assignments, including the band centers, maximum J and K_a values of observed transitions, the numbers of assigned transitions and determined energy levels, are given in Table 2. For illustration, some examples of assigned transitions are also shown in Figs. 2 and 3.

The rotational energy levels of the four upper states were obtained from the assignments and are listed in Table 3. Most of the energy levels were determined by more than two transitions from different ground state levels. Δ, the experimental uncertainties in 10^{-4} cm^{-1}, are also presented in the same table. For most levels, Δ values are less than 0.002 cm^{-1}, which represent the experimental accuracy.

The Watson type Hamiltonian [37] was used to fit the experimental energy levels:

$$
\begin{aligned}
H^v = {} & E^v + [A^v - \tfrac{1}{2}(B^v + C^v)]J_z^2 + \tfrac{1}{2}(B^v + C^v)J^2 \\
& + \tfrac{1}{2}(B^v - C^v)J_{xy}^2 - \Delta_K^v J_z^4 - \Delta_{JK}^v J_z^2 J^2 - \Delta_J^v J^4 \\
& - \delta_K^v[J_z^2, J_{xy}^2]_+ - 2\delta_J^v J^2 J_{xy}^2 + H_K^v J_z^6 + H_{KJ}^v J_z^4 J^2 \\
& + H_{JK}^v J_z^2 J^4 + H_J^v J^6 + [J_{xy}^2, h_K^v J_z^4 + h_{JK}^v J^2 J_z^2 \\
& + h_J^v J^4]_+ + L_K^v J_z^8 + L_{KKJ}^v J_z^6 J^2 + L_{JK}^v J_z^4 J^4 \\
& + L_{KJJ}^v J_z^2 J^6 + L_J^v J^8 + [J_{xy}^2, l_K^v J_z^6 + l_{KJ}^v J^2 J_z^4 \\
& + l_{JK}^v J^4 J_z^2 + l_J^v J^6]_+ + P_K^v J_z^{10} + [J_{xy}^2, p_K^v J_z^8]_+ \\
& + \cdots,
\end{aligned}
\tag{3}
$$

where $J_{xy}^2 = J_x^2 - J_y^2$ and $[A, B]_+ = AB + BA$. The results of the fitted parameters with their standard deviation values of 1σ statistical confidence intervals are presented in Table 4. Column 2 presents the values of corresponding parameters of the ground vibrational state, Columns 3–6 present the set of fitted parameters. In Table 3, the differences between experimentally determined energies and calculated values, $\delta = E^{\mathrm{exp}} - E^{\mathrm{cal}}$ in $10^{-4}\ \mathrm{cm}^{-1}$, are also presented. It can be found that they are very close to the corresponding experimental uncertainty values Δ. Note that these levels can be well reproduced by the Hamiltonian Eq. (3) for an isolated vibrational state.

The derived values of the rotational constants A, B, and C in Table 4 allow the estimation of the rotation–vibration coefficients α_i^γ from the formula

$$
P^\gamma = P_0^\gamma - \sum_{i=1}^{3} \alpha_i^\gamma v_i,
\tag{4}
$$

where P^γ is one of the rotational constants, A, B, and C for $\gamma = z$, x, y, respectively. With available rotational parameters of 13 experimentally determined states

Table 5
Vibration–rotation coefficient α_i^γ of the HD^{32}S molecule (in cm^{-1})[a]

	Calc.[b]	Exp.[c]
α_1^z	0.0000	0.0[d]
α_2^z	−0.267	−0.290(6)
α_3^z	0.2967	0.2921(47)
α_1^x	0.1001	0.1004(18)
α_2^x	−0.097	−0.098(1)
α_3^x	0.0000	0.0[d]
α_1^y	0.0387	0.0391(3)
α_2^y	0.028	0.0344(2)
α_3^y	0.0291	0.0300(1)

[a] Values in parentheses are the 1σ statistical confidence intervals.
[b] Calculated values from [26,27].
[c] Fitted with rotational constants of 13 bands from this work and [23–27].
[d] Constrained to zero.

Table 4
Spectroscopic parameters of the (002), (012), (003), and (013) vibrational states of the HD^{32}S molecule (in cm^{-1})[a]

	(000)[b]	(002)	(012)	(003)	(013)
E	—	5147.35541(40)	6139.73166(37)	7577.84116(45)	8548.89130(70)
A	9.75178412	9.1778264(621)	9.4293850(494)	8.891950(106)	9.131920(200)
B	4.93213844	4.9327828(198)	5.0294614(265)	4.9331788(373)	5.0322481(581)
C	3.22570284	3.1665462(164)	3.1319955(115)	3.1357068(156)	3.1010413(301)
$\Delta_K \times 10^3$	−0.377125	−0.39004(243)	−0.33479(185)	−0.42232(409)	−0.3093(171)
$\Delta_{JK} \times 10^3$	0.956467	0.94471(152)	1.03023(106)	0.94248(256)	1.02585(366)
$\Delta_J \times 10^3$	0.087209	0.0881695(945)	0.101408(138)	0.088688(186)	0.102229(309)
$\delta_K \times 10^3$	0.648383	0.635474(856)	0.805406(747)	0.63132(208)	0.78369(276)
$\delta_J \times 10^3$	0.0284447	0.0293044(324)	0.0360416(746)	0.029772(105)	0.036651(155)
$H_K \times 10^6$	0.4191	0.6222(387)	0.8538(319)		1.730(350)
$H_{KJ} \times 10^6$	−0.6773	−0.8076(270)	−1.2115(190)	−1.0262(695)	−1.092(123)
$H_{JK} \times 10^6$	0.43313	0.4391(108)	0.63681(442)	0.4915(243)	0.5587(250)
$H_J \times 10^6$	0.002307	0.002212(172)	0.004123(359)	0.001946(144)	0.001866(544)
$h_K \times 10^6$	0.9932	0.91152(964)	1.4301(254)	0.9474(588)	1.0282(904)
$h_{JK} \times 10^6$	0.20978	0.21295(421)	0.28749(349)	0.2283(122)	0.2249(139)
$h_J \times 10^6$	0.001199		0.001959(188)		
$L_K \times 10^9$	−2.655	−3.887(165)	−4.082(222)		
$L_{KKJ} \times 10^9$	−1.189	−1.186(128)	−1.9393(963)		
$L_{KJ} \times 10^9$	3.760	4.362(169)	5.934(252)		
$L_{KJJ} \times 10^9$	−0.1201	−0.1108(294)			
$l_K \times 10^9$	−1.722		−2.761(261)		
$l_{KJ} \times 10^9$	−0.479		−0.6029(619)		
$l_{JK} \times 10^9$	−0.0656				
$P_K \times 10^{12}$	0.2922				
$p_K \times 10^{12}$	−6.43				
$\sigma \times 10^3$		1.40	1.37	1.42	2.08

[a] Values in parentheses are the 1σ statistical confidence intervals. Values of parameters presented in columns 3–6 without confidence intervals were constrained to the values of corresponding parameters of the ground state (in column 2).
[b] Reproduced from [2].

including four states in present work and those in [23–27], the rotation–vibration coefficients α_i^γ ($i = 1,2,3$) were obtained by a least square fitting. The results are presented in Table 5. In the fitting, α_1^z and α_3^x were constrained to zero because they cannot be determined well due to limited available experimental data. In [26,27], the parameters α_i^γ were also estimated with the isotope substitution method. For comparison, these values are also presented in Table 5. One can find a satisfactory agreement between them.

Due to the symmetry of the HDS molecule, each vibrational band should be a hybrid band with both 'A' and 'B' type transitions. The strengths of those ro-vibrational transitions can help to determine the vibrational transition dipole moment, which can be compared with the results given by ab initio calculations [32]. Even the relative linestrengths can be very helpful for such study. For example, the relative intensity of the 'A' and 'B' type transitions to a same upper level can help to determine the direction of the vibrational transition dipole moment vector. For this purpose, we also tried to determine the relative linestrengths in the bands studied in present work. In Table 6, all the transitions to the $J' = 3$ upper levels are presented.

Table 6
Relative linestrengths for the $J' = 3$ transitions in the $2v_3$, $v_2 + 2v_3$, $3v_3$, and $v_2 + 3v_3$ bands

J'	K_a'	K_c'	J''	K_a''	K_c''	$2v_3$		$v_2 + 2v_3$		$3v_3$		$v_2 + 3v_3$	
						v (cm^{-1})	$I_{\rm rel}$	v (cm^{-1})	$I_{\rm rel}$	v (cm^{-1})	$I_{\rm rel} \times 100$	v (cm^{-1})	$I_{\rm rel} \times 100$
3	0	3	2	0	2	5169.7833	1.00	6162.3247	2.05	7599.9158	4.17	8571.1344	4.28
			4	0	4	5117.1109	0.90	6109.6521	2.17	7547.2476	3.14	8518.4724	5.74
			2	1	2	5166.2945	4.56	6158.8350	0.09	7596.4318	4.88	—	—
			3	1	2	5134.4385	3.70	6126.9812	0.12	7564.5765	4.39	—	
			4	1	4	5116.0121	4.58	6108.5529	0.11	7546.1498	4.77	—	—
3	1	2	2	1	1	5173.3291	1.04	6166.6532	2.06	7603.4233	9.59	8575.4230	4.06
			3	1	3	5156.7465	0.19	6150.0692	0.48	7586.8275	1.19	8558.8323	1.41
			4	1	3	5111.5049	0.82	6104.8279	2.16	7541.5968	3.36	8513.5990	4.12
			3	0	3	5158.8639	4.29	6152.1867	0.10	7588.9576	4.77	—	—
			3	2	1	5132.6623	4.42	6125.9869	0.10	7562.7534	5.09	—	—
			4	2	3	5102.1472	2.87	—	—	7532.2389	3.14	—	—
3	1	3	2	1	2	5167.9377	1.05	6160.4893	1.99	7597.8560	2.76	8569.0699	3.90
			3	1	2	5136.0846	0.30	6128.6336	0.42	7565.9963	0.87	8537.2149	1.35
			4	1	4	5117.6562	0.99	6110.2078	2.22	7547.5745	3.09	8518.7942	5.80
			2	0	2	5171.4258	4.93	6163.9790	0.10	7601.3443	5.42	—	—
			3	2	2	5123.9351	2.09	—	—	7553.8538	2.82	—	—
			4	0	4	5118.7546	4.12	6111.3048	0.13	7548.6727	4.06	—	—
			4	2	2	5086.8868[a]	1.29[a]	—	—	7516.7890	1.41	—	—
3	2	1	2	2	0	5170.9510	0.85	6164.7829	1.12	7600.3363	1.73	8572.8202	2.55
			3	2	2	5146.8871	0.65	6140.7177	1.29	7576.2725	1.84	8548.7556	2.76
			4	2	2	5109.8102[b]	2.25[b]	6103.6569	1.53	7539.2111	2.38	8511.6932	3.36
			2	1	2	5190.8905	1.74	—	—	7620.2737	1.95	—	—
			3	1	2	5159.0352	4.46	6152.8669	0.10	7588.4203	4.60	—	—
			3	3	0	5118.2908	2.03	—	—	7547.6742	2.38	—	—
			4	3	2	5085.1894	3.50	6079.0209	0.08	7514.5732	3.85	—	—
3	2	2	2	2	1	5169.2663	0.61	6162.8911	1.32	7598.4898	1.79	8570.7465	2.76
			3	2	1	5143.0518	0.59	6136.6818	2.85	7572.2719	1.95	8544.5338	2.93
			4	2	3	5112.5358	0.87	6106.1606	1.55	7541.7541	2.49	8514.0218	3.25
			2	1	1	5183.7195	2.94	—	—	7612.9391	3.68	—	—
			3	1	3	5167.1298[c]	4.54[c]	—	—	7596.3570	2.60	—	—
			3	3	1	5116.2822	1.57	—	—	7545.5050	2.28	—	—
			4	1	3	5121.9002	4.16	—	—	7551.1161	1.25	—	—
			4	3	1	5082.7659	3.62	—	—	7623.1000	4.33	—	—
3	3	0	3	3	1	5142.2118	1.13	6136.9643	2.91	7570.1148	3.74	8543.4397	5.47
			4	3	1	5108.6944	0.46	6103.4484	0.81	7536.5984	1.35	8509.9287	2.22
			2	2	1	5195.1968	3.46	—	—	7623.1000	4.33	—	—
			3	2	1	5168.9807	1.81	—	—	7596.8833	1.90	—	—
			4	4	1	5069.9509	3.71	—	—	7497.8542	4.82	—	—
3	3	1	3	3	0	5142.0865	1.24	6136.8290	2.91	7569.9764	3.90	8543.2904	5.80
			4	3	2	5108.9861	0.43	6103.7282	0.87	7536.8767	1.30	8510.1924	2.00
			2	2	0	5194.7482	3.74	—	—	7622.6382	4.55	—	—
			3	2	2	5170.6835	1.39	—	—	7598.5771	2.06	—	—
			4	4	0	5069.8730	4.68	6064.6147	0.10	7497.7644	5.09	—	—

[a] Blended by transition [10 4 7] ← [10 5 6].
[b] Blended by transition [7 3 4] ← [7 4 3].
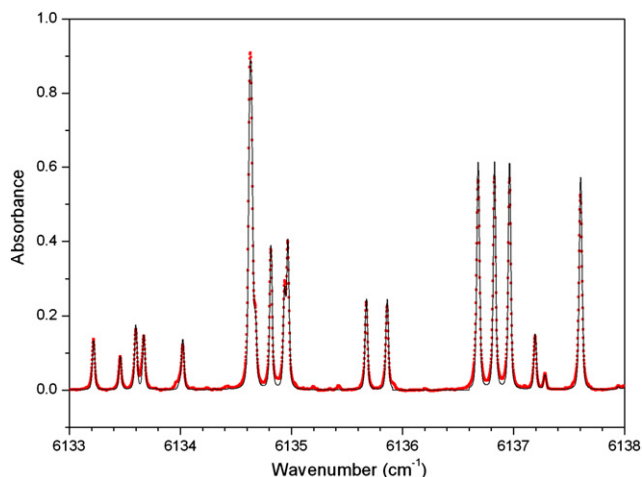[c] Blended by transition [4 3 1] ← [4 2 2].

Fig. 4. The simulated (in solid line) and observed (in scatter points) spectrum of HDS in the 6133–6138 cm^{-1} region.

The relative linestrengths values were derived from the absorbance of each line and normalized to the experimental path length and gas pressure, finally compared with the first transition in that table, $[3_{03} \leftarrow 2_{02}]$ line of the $2\nu_3$ band. Several weak transitions with $\Delta K_a = \pm 1$, $\Delta K_c = \pm 3$ of $2\nu_3$ band are also observed, but not included in the fitting.

The relative intensity of the 'A' and 'B' type transitions are about 1:4 and 1:2 for $2\nu_3$ and $3\nu_3$ bands, respectively. And the number of the assigned 'A' and 'B' type transitions are 283, 602 and 191, 325 for these two bands, respectively. While for the $\nu_2 + n\nu_3$ ($n = 2, 3$) bands, the strengths of the 'A' type transitions are close or even stronger than the corresponding transitions of the $n\nu_3$ bands, but the corresponding 'B' type transitions are much weaker (or even unobservable in present spectrum). With the preliminary information on the vibrational transition dipoles retrieved from the relative linestrengths and the ro-vibrational parameters presented in Table 4, we can produce a simulation of the spectrum. In Fig. 4, a small portion of the simulated $\nu_2 + 2\nu_3$ band spectrum together with the observed one are given. The excellent agreement also indicates that this is a well-isolated band. With the summary of all the linestrengths given in Table 6 for each vibrational band, we can also get some information on the relative band intensities. They are $I_{002}:I_{012}:I_{003}:I_{013} = 149:51:2:1$, which agree well with the values 77:22:4:1 given by ab initio calculation [38]. We hope these results would be used to check succeeding more accurate ab initio study on this molecule.

References

[1] C. Vastel, T.G. Phillips, C. Ceccarelli, J. Pearson, Astrophys. J. 593 (2003) L97–L100.
[2] J.-M. Flaud, C. Camy-Peyre, J.W.C. Johns, Can. J. Phys. 61 (1983) 1462–1473.
[3] K.M.T. Yamada, S. Klee, J. Mol. Spectrosc. 166 (1994) 395–405.
[4] A.H. Saleck, M. Tanimoto, S.P. Belov, T. Klaus, G. Winnewisser, J. Mol. Spectrosc. 171 (1995) 481–493.
[5] C. Camy-Peyret, J.-M. Flaud, L. Lechuga-Fossat, J.W.C. Johns, J. Mol. Spectrosc. 109 (1985) 300–333.
[6] S.P. Belov, K.M.T. Yamada, G. Winnewisser, L. Poteau, J. Demaison, O. Polyansky, M.Yu. Tretyakov, J. Mol. Spectrosc. 173 (1995) 380–390.
[7] O.N. Ulenikov, A.B. Malikova, M. Koivusaari, S. Alanko, R. Anttila, J. Mol. Spectrosc. 176 (1996) 229–235.
[8] O.N. Ulenikov, G.A. Onopenko, M. Koivusaari, S. Alanko, R. Anttila, J. Mol. Spectrosc. 176 (1996) 236–250.
[9] O.N. Ulenikov, A.-W. Liu, E.S. Bekhtereva, O.V. Gromova, L.-Y. Hao, S.-M. Hu, J. Mol. Spectrosc. 226 (2004) 57–70.
[10] O.N. Ulenikov, A.-W. Liu, E.S. Bekhtereva, S.V. Grebneva, W.-P. Deng, O.V. Gromova, S.-M. Hu, J. Mol. Spectrosc. 228 (2004) 110–119.
[11] O.V. Zotov, V.S. Makarov, O.V. Naumenko, A.D. Bykov, Atmospheric Opt. 4 (1991) 798–806.
[12] L. Lechuga-Fossat, J.-M. Flaud, C. Camy-Peyret, P. Arcas, M. Cnisenier, Mol. Phys. 61 (1987) 23–32.
[13] L.R. Brown, J.A. Crisp, D. Crisp, O.V. Naumenko, M.A. Smirnov, L.N. Sinitsa, A. Perrin, J. Mol. Spectrosc. 188 (1998) 148–174.
[14] J.-M. Flaud, R. Großkloß, S.B. Rai, R. Stuber, W. Demtröder, D.A. Tate, L.-G. Wang, Th.F. Gallagher, J. Mol. Spectrosc. 172 (1995) 275–281.
[15] J.-M. Flaud, O. Vaittinen, A. Campargue, J. Mol. Spectrosc. 190 (1998) 262–268.
[16] M.S. Child, O.V. Naumenko, M.A. Smirnov, L.R. Brown, Mol. Phys. 92 (1997) 885–893.
[17] A.D. Bykov, O.V. Naumenko, M.A. Smirnov, L.N. Sinitsa, L.R. Brown, J. Crisp, D. Crisp, Can. J. Phys. 72 (1994) 989–1000.
[18] O. Vaittinen, L. Biennier, A. Campargue, J.-M. Flaud, L. Halonen, J. Mol. Spectrosc. 184 (1997) 288–299.
[19] O. Naumenko, A. Campargue, J. Mol. Spectrosc. 209 (2001) 242–253.
[20] O. Naumenko, A. Campargue, J. Mol. Spectrosc. 210 (2001) 224–232.
[21] Y. Ding, O. Naumenko, S.-M. Hu, Q.S. Zhu, E. Bertseva, A. Campargue, J. Mol. Spectrosc. 217 (2003) 222–238.
[22] C. Camy-Peyret, J.M. Flaud, A. N'Gom, J.W.C. Johns, Mol. Phys. 65 (1988) 547–649.
[23] O.N. Ulenikov, R.N. Tolchenov, E.N. Melekhina, M. Koivusaari, R. Anttila, J. Mol. Spectrosc. 170 (1995) 397–416.
[24] C. Camy-Peyret, J.M. Flaud, A. N'Gom, J.W.C. Johns, Mol. Phys. 67 (1989) 693–695.
[25] O.N. Ulenikov, R.N. Tolchenov, M. Koivusaari, S. Alanko, R. Antilla, J. Mol. Spectrosc. 170 (1995) 1–9.
[26] O.N. Ulenikov, E.A. Ditenberg, I.M. Olekhnovitch, S. Alanko, M. Koivusaari, R. Anttila, J. Mol. Spectrosc. 191 (1998) 239–247.
[27] O.N. Ulenikov, G.A. Onopenko, I.M. Olekhnovitch, S. Alanko, M. Koivusaari, R. Anttila, J. Mol. Spectrosc. 189 (1998) 74–82.
[28] L. Halonen, T. Carrington Jr, J. Chem. Phys. 88 (1988) 4171–4185.
[29] I.N. Kozin, P. Jensen, J. Mol. Spectrosc. 163 (1994) 483–509.
[30] O. Polyansky, P. Jensen, J. Tennyson, J. Mol. Spectrosc. 178 (1996) 184–188.

[31] Vl.G. Tyuterev, S.A. Tashkun, D.W. Schwenke, Chem. Phys. Lett. 348 (2001) 223–234.

[32] Vl.G. Tyuterev, L. R'egalia-Jarlot, D.W. Schwenke, S.A. Tashkun, Y.G. Borkov, C. R. Phys. 5 (2004) 189–199.

[33] T. Cours, P. Rosmus, Vl.G. Tyuterev, Chem. Phys. Lett. 331 (2000) 317–322.

[34] T. Cours, P. Rosmus, Vl.G. Tyuterev, J. Chem. Phys. 117 (2002) 5192–5208.

[35] G. Tarczay, A. Csaszar, M. Leininger, W. Klooper, Chem. Phys. Lett. 322 (2000) 119–128.

[36] L.S. Rothman, A. Barbe, D. Chris Benner, L.R. Brown, C. Camy-Peyret, M.R. Carleer, K. Chance, C. Clerbaux, V. Dana, V.M. Devi, A. Fayt, J.-M. Flaudi, W.J. Lafferty, J.-Y. Mandin, S.T. Massie, V. Nemtchinov, D.A. Newnham, A. Perrin, C.P. Rinsland, J. Schroeder, K.M. Smith, M.A.H. Smith, K. Tang, R.A. Toth, J. Vander Auwera, P. Varanasi, K. Yoshino, J. Quant. Spectrosc. Radiat. Transfer 82 (2003) 5–44.

[37] J.K.G. Watson, J. Chem. Phys. 46 (1967) 1935–1949.

[38] S. Miller, J. Tennyson, P. Rosmus, J. Senekowitsch, I.M. Mills, J. Mol. Spectrosc. 143 (1990) 61–80.